Reaction and Transport in Industrial-Scale Fixed Bed Transactelyzation of Glycerol

A Major Qualifying Project Report

Submitted to the Faculty of the
WORCESTER POLYTECHNIC INSTITUTE

In partial fulfillment of the major requirements for the Degree of Bachelor of Science in Chemical Engineering

By

Hoang Chi Duc

April 2018

Contents

Abstract

The rise of biodiesel production has its downside in producing an abundance of glycerol as a by-product. The project examines the feasibility of converting glycerol to glycerol acetate, a much more valuable product, through transactelyzation of glycerol. The project utilized COMSOL Multiphysics to simulate the process on Amberlyst -15 catalyst and in fixed bed reactor. The model evaluated all physical phenomena that may happen in industrial-scale process. The simulation allowed proposing design recommendation for the fixed bed reactor. The result shows that fixed bed reactor is feasible for processing transactelyzation of glycerol.

2. Introduction

One major concern with biodiesel production is the amount of by-product it produces. For every 9 kg (19.8 lbs) of biodiesel produced, about 1 kg (2.2 lbs) of a crude glycerol by-product is formed [1]. While refining the crude glycerol is an option, glycerol is inconsequential in the chemical industry. This solution is deemed as uneconomically. Therefore, it is necessary to convert crude glycerol into more valuable product. Traditional chemist has already taken an interest on the matter and multiple studies have been conducted to figure out a pathway for crude glycerol conversion. The proposed method included converting glycerol to ethanol, methanol or treated by appropriate method to utilize as food for livestock. The method that is in the scope of this paper is the chemical conversion of glycerol into glycerol acetate by liquid-phase transacetylization of glycerol. Glycerol acetate can be used as a fuel additive. Adding glycerol acetates to biodiesel has been found to reduce particulate emissions, pour point and viscosity at low temperatures [2]. Equation 1 shows the main reaction to produce glycerol acetates:

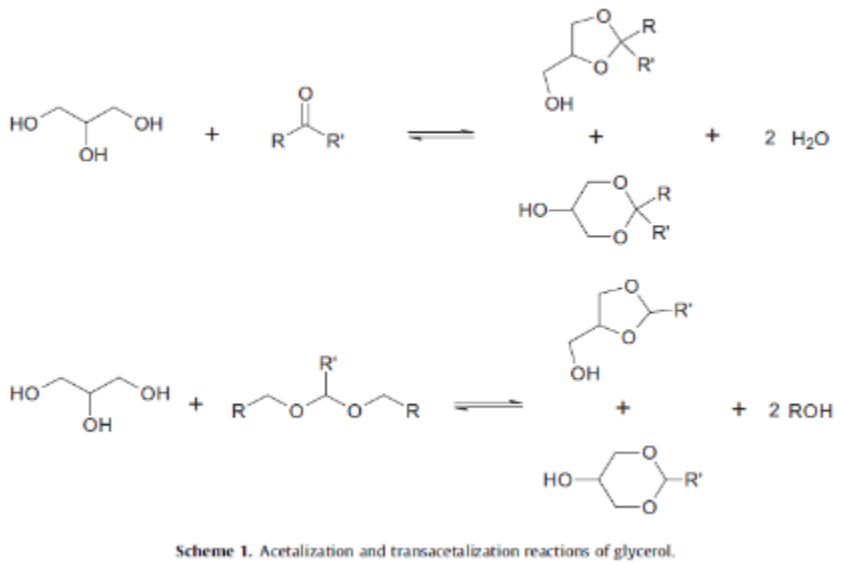

Scheme 1. Acetalization and transacetalization reactions of glycerol.

Figure 1: Transactelyzation of Glycerol [3]

The kinetic model of the chemical reaction has been well-studied. Hong et al[3] proposed a simple but accurate kinetic model that agrees with previous study, confirming the consistency of the experiment. The model predicts that the forward reaction will have favorable yield at

reasonable conditions, which make it suitable for industrial purpose. The ideal condition, according to the paper, was under 50 C to avoid the formation of side products[3]. However, the behavior of the reaction in an industrial scale reactor has not yet been investigated. The paper will unveil the efficacy of liquid-phase transacetylization of glycerol in such reactor. The focus of the paper is a fixed bed reactor as it is one of the most common types of reactor. The paper will study the kinetics of the reaction in fixed bed reactor. Diffusion limitation, temperature gradient, mass and heat transfer will be considered. Understanding of the process allows the optimization of the reactor. Recommendations about design of the reactor will be made to as a result of the optimization process.

COMSOL Multiphysics is used to simulate the chemical process in the fixed bed reactor model. From literature, it is known that while the diffusion and heat transfer take part along the reactor, the reaction happens only in catalyst pellet. The model is divided into two sub-model to reflect the phenomenon. One mode-l is account for the environment outside of the pellet but inside the reactor, where both the heat transfer and mass transfer process exist. Another model is account for the physical and chemical process inside the catalyst pellet. The program will consider the interaction between the two models as well as the result of each independent model to make the final calculation.

The result of the simulation confirms liquid-phase transacetylization of glycerol as a feasible solution for excess crude glycerol in biodiesel industry with high yield, acceptable quality at reasonable reactor condition.

3. Background

3.1 Overview on biodiesel production

Fossil fuel raises many concerns about environment in the last few years. As such, several alternative energy sources were looked at as potential replacement. These energy sources have the same advantages of being friendly to the environment. The list includes but not limited to solar energy, wind energy, biodiesel, nuclear energy. Of the list, biodiesel appears to be the most attractive solution as wind energy or solar depends excessively on weathers to be reliable, while nuclear power is a time bomb in most situations. Therefore, it is no surprise that biodiesel

production in US has reached a new height. By 2016, the volume of biodiesel produced in US passed the mark of 1.5 billion gallons. It is a remarkable achievement, considering the industry is almost non-existent merely 15 years ago. Much of the success is owed to political agenda of the US government with multiple policy issued by EPA to encourage biodiesel production [4].

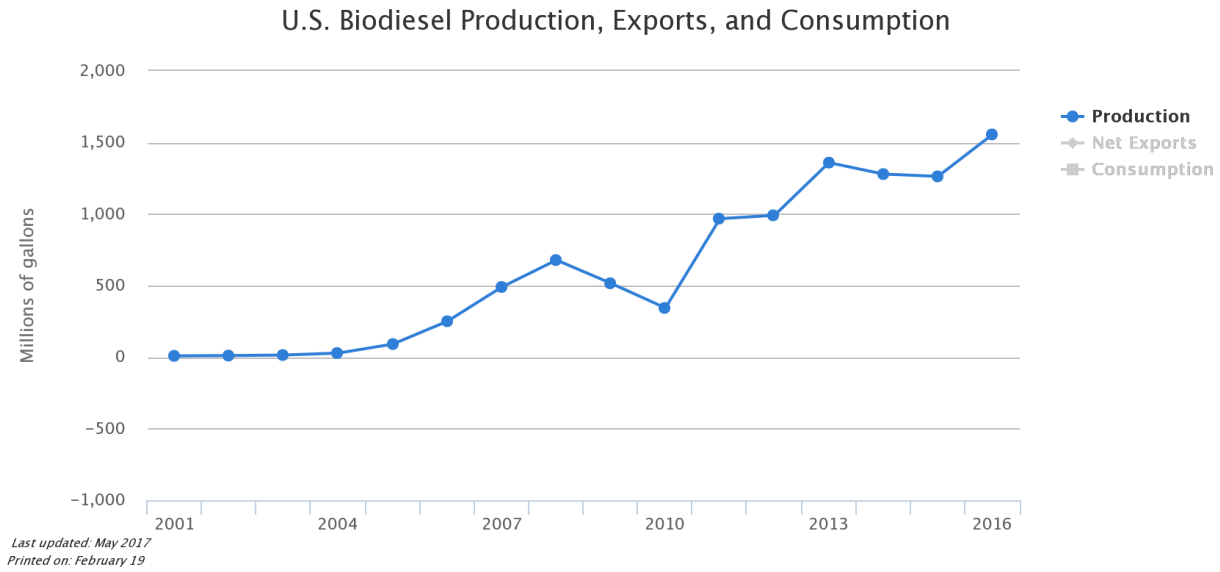

Figure 3-1: U.S Biodiesel Production in 21st century[5]

The main raw input into biodiesel reactor is sunflower oil. Other biodiesel unit also employs animal fat as input but it is less likely due to higher cost[6]. The main component of sunflower oil and animal fat is triglyceride. Triglyceride belongs to the ester class of organic compound as it has three carboxylic acid covalent bonded to glycerol. These three carboxylic acids go through another esterification with alcohol (methanol or ethanol) to form biodiesel (**Figure 3-1)**. This type of reaction is classified as transesterification where ester is converted to a different ester through exchange of the alkoxy functional group. When one of the reactants is alcohol, the reaction is also known as alcoholysis.

Transesterification is an equilibrium reaction that heavily relies on a catalyst to progress. Catalyst currently in used is alkali, acid or biocatalyst. To drive the reaction forward, the common practice is to put alcohol in excess. The reaction stoichiometry require 3 mol alcohol for each mol of triglycerides but industrial process uses 6 mol alcohol per mol of triglyceride instead. The result is a yield of 98 % minimum on weight basis for esters product.

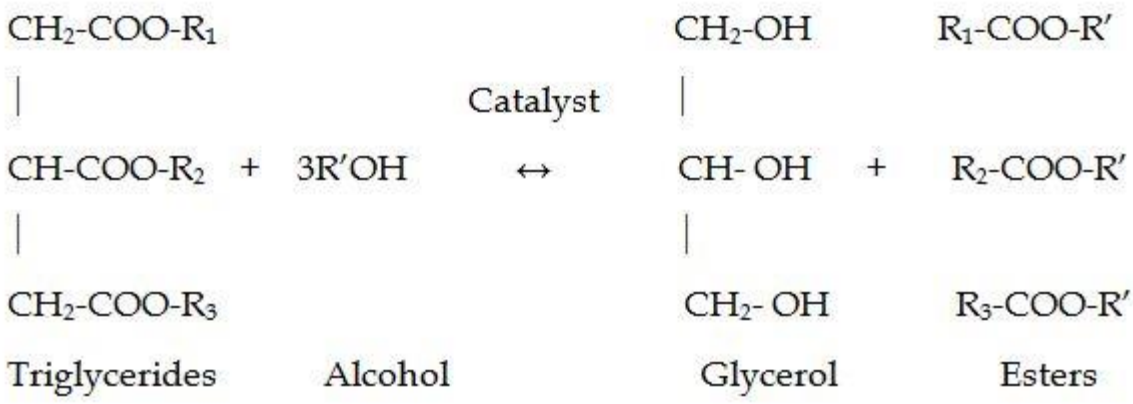

Transesterification of lipid and alcohol[7]

Crude glycerol is the most significant by-product. Crude glycerol as biodiesel by-product contains 38 to 92% glycerol while the rest is methanol and soap[8]. The fluctuated quality of glycerol combined with high level of impurities limit the use of crude glycerol in industry. Refining crude glycerol is not beneficial since glycerol is not a valuable chemical. Crude glycerol is hard to dispose of and can potentially become a pollutant source. As the biodiesel industry is projected to grow steadily in the future, it is important to find a solution to crude glycerol.

3.2. Utilize by-product glycerol.

Crude glycerol can be used as feed for livestock as the price of corn is sky high while there is an excess amount of crude glycerol. Livestock's liver can convert crude glycerol to glucose at extraordinary rate by enzyme glycerol kinase. However, the downside of this approach is excess glycerol in livestock might cause psychology symptom. Pig and hen show normal growth at the intake of 2.5% to 10% crude glycerol but show poor feed flow at the intake level above 10%. Controlling the intake of actual glycerol for livestock proves to be difficult as the quality of crude glycerol varies. Crude glycerol impurities contain methanol so consuming it may prove to be fatal to livestock. The metabolism of glycerol create high level of potassium, which may disrupt the electrolyte imbalance in livestock.[9]

Crude glycerol can go through biological conversion to valuable chemical. One of the most promising option is to use a fed batch culture of *Klebsiella pneumonia* to produce 1, 3-propanediol. The procedure has a low fermentation cost with high yield. The optimized process output is 56g/L in yield with a purity of 99% and recovery of 34%[10]. However, biological conversion require strict condition as the bacteria is vulnerable to temperature change which make it not feasible for industrial purpose.

Combustion is a potential solution for crude glycerol as its boiling can generate steam and electricity. Combining the process with biodiesel production may lead to energy optimization, reducing gas emission, eliminating transportation cost. Study shows that despite inferior property such as high viscosity, high autoignition temperature and low heating value, crude glycerol can be used to produce 100% glycerol flame [11]. The combustion, however, also emits unsaturated aldehyde, a substance with acrid smell and highly toxic. The combustion also leaves large amount of sodium and phosphorous derived from catalyst, which reduce the purity of the product.

Hydrogen production via steam reforming glycerol in packed bed reactor is also a possible solution for the abundance of glycerol. Detail process was examined by MacDonald and Olm [12], who found that the process is viable for industrial-scale with reasonable conversion. Packed bed reactor was stated to be a suitable reactor style for steam reforming. Bimetallic Ni–Co/Al2O3 is used as catalyst for the heterogeneous reaction. The downside of the process is the possibility of side-reaction such as water-gas shift or methannation which may reduce quality of the product. The reaction is diffusion limited and while it was confirmed that the diffusion limitation doesn't have profound effect on the process, it is desired to have another chemical pathway to bypass this barrier.

3.3 Glycerol acetate

Crude glycerol can be converted to glycerol acetate through liquid-phase transacetylization of glycerol. Study shows that adding glycerol acetate to biodisel reduce particulate emissions, pour point and viscosity at low temperatures. Glycerol acetate has the advantage of being produced and used on-site with biodisel production, bypassing the cost of transportation. The

reaction kinetics have been studied in detailed by *Hong et al [3]*. As such, there is a desire to design chemical process for liquid-phase transacetylization of glycerol in industrial-scale.

3.4 Transacetalization of glycerol

3.4.1 Overview

Transacetalization of glycerol converts glycerol to glycerol acetate by alcoholysis with ethanol as reactant and Amberlyst-15 as catalyst. As for most catalytic reactions, the reaction follows 7 steps [13] :

1. Diffusion of the reactants from the bulk fluid to the external surface of the catalyst pellet

2. Diffusion of the reactant from the pore mouth through the catalyst pores to the immediate vicinity of the internal catalytic surface

3. Adsorption of reactants onto the catalyst surface

4. Reaction on the surface of the catalyst.

5. Desorption of the products from the surface

6. Diffusion of the products from the interior of the pellet to the pore mouth at the external surface

7. Mass transfer of the products from the external pellet surface to the bulk fluid

The paper will aim to explore which is the limiting step of the reaction.

The reaction will be simulated in a cylindrical-tube fixed bed reactor filled with porous, solid catalyst pellet. The catalyst is held in place during the process while the reactant in liquid phase flows through. Transacetalization of glycerol has a low heat of reaction (~20.5kJ/mol) so adiabatic reactor is assumed[3]. The adiabatic reactor is insulated by a cylindrical jacket surrounding the core. The jacket can be made by several layer of platinum or silver wire[13].

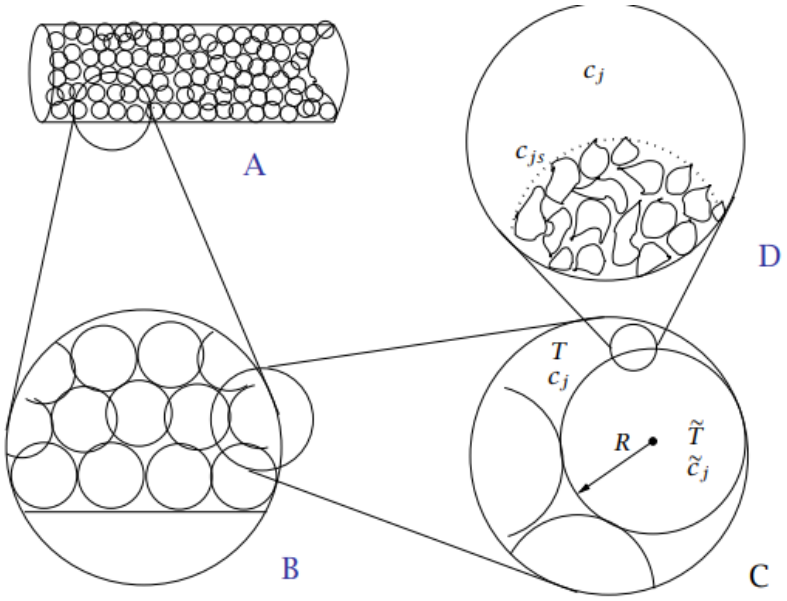

Figure 3-1: Expand view of fixed bed reactor.[14]

The overall reaction of transacetalization of glycerol is shown below:

$$C_3H_8O_3 + C_6H_{14}O_2 \rightarrow 2C_2H_6O + C_7H_{10}O_3$$

If the reaction is conducted below 50 C, there is no side reaction. The main reaction is reversible but study claimed that the forward reaction is dominant[12]. The simulation will take the reversible reaction into account nonetheless.

The desired product includes s, the cis- and trans-forms of 5-hydroxy-2-methyl-1,3- and 4-hydroxymethyl-2-methyl-1,3-dioxolane. The products can be used as fuel addictive for the biodiesel reactor so it might be possible to connect the product stream to biodiesel reactor to utilize the product immediately. This method has the advantage of bypassing transportation cost so no logistic infrastructure is required to be invested.

3.4.2 Mass transfer:

The mass transfer process happens in steps 1,2,6 and 7 listed above. Step 1 and 7 represent external diffusion as reactant diffuse between pellet surface and the bulk flow. Step 2 and 6 represent internal diffusion as reactant diffuse between interior of the pellet and its surface. External diffusion shall be considered first.

The rate N (mol cm−2 s−1) of mass transfer of a liquid-phase reactant through the external surface of the pellet is given by :

$$N = k_c (c_0 - c_s).$$

c_O (mol cm^-3) is the concentration of reactant at the bulk liquid while c_S is the concentration at the surface. K_C is the mass transfer coefficient and N is the molar flux. The value of k_C is calculated using the Sherwood number.

$$Sh = k_c D_p / D$$

D_P is the catalyst particle diameter (cm), D (cm2 s−1) is the diffusion coefficient of the reactant and Sh is the Sherwood number, calculated using the following formula

$$Sh = 2 + 1.1 Re^{0.6} Sc^{1/3}$$

Re is the Reynolds number and Sc is the Schmidt Number, given by the following equation

$$Re = \frac{\rho D V}{\mu}$$

$$Sc = \frac{\mu}{\rho D_{AB}}$$

The multicomponent liquid diffusion coefficient is calculated using the Wilke- Chang correlation:

$$D = 7.4 \times 10^{-8} \frac{(xM)^{1/2} T}{\eta V^{0.6}}$$

where T is the absolute temperature, M the molecular weight, η the viscosity, and V the molar volume at the normal boiling point.

Internal diffusion is displayed by step 2 and step 6 of the reaction. The diffusion rate is calculated using Fick's law :

$$N_i = -D_e\left(\frac{\partial c}{\partial z}\right)$$

D_e is the effective diffusion coefficient while $\partial w/\partial z$ is the concentration gradient. D_e is calculated using the following equation:

$$D_e = D * \varepsilon/\tau$$

ε is the porosity of the catalyst pellet and τ is the tortuosity of the catalyst pellet. Porosity measures the void space inside the reactor while tortuosity measures the catalyst pellet porous structure. For diffusion process, porosity promotes diffusion since a large value of porosity means more space for diffusion process to occur. Tortuosity, on the other hand, hinders the diffusion process. The modified D_e accounts for the effect of porous catalyst on the mass transfer process. For Amberlyst 15, the porosity is given to be 0.44 and tortuosity is 0.4[16]

The effective diffusivity is calculated for each component of the reaction and shown in the table 3-1 below.

Component	Effective diffusivity (m2/s)
Glycerol	3.07E-09
Ethanol	2.92E-09
Glycerol acetate	1.94E-09
C6H14O2	5.58E-11

Table 3.1:Effective diffusivity of components of the mixture

To determine if internal diffusion is the limitation step, the effectiveness factor is calculated by the following formula:

$$\eta = \frac{\text{actual overall rate of reaction}}{\text{rate of reaction at surface}}$$

3.4.3 Pressure drop

The reaction kinetics are not dependent on partial pressure as the reaction happens in liquid phase, but pressure drop is still of concern due to its effect on flow distribution, pumping power, and operational cost of the reactor. Ergun equation is used to calculate pressure drop in packed bed reactor:

$$\frac{dP}{dz} = -\frac{G}{\rho d_p}\left(\frac{1-\varphi}{\varphi^3}\right)\left[150\frac{(1-\varphi)\mu}{d_p} + 1.75G\right]$$

P represents pressure (Pa), z represents the length of the packed bed (m), φ represents the bed voidage ($volume\ of\ reactor - volume\ of\ catalyst\ particles)/\ volume\ of\ reactor$), G represents the mass flux (kg/m2 s), dp represents the catalyst pellet diameter (m), μ represents the fluid viscosity (kg/m s), and ρ is the fluid density (kg/m3).

3.4.4 Heat transfer:

Transacetalization of glycerol is an exothermic reaction so the temperature of the bulk flow is expected to increase along the reactor length. As such, the reacting condition is not isothermal and there is heat transfer process inside the reactor. Heat transfer can appear under three forms : conduction, convection and radiation[14]. Radiation occurs at high wall temperature and is neglected because the reactor is operated at low temperature. The bulk fluid provides a means for convective heat transfer between the wall and the particle while the particles transfer heat to each other by conduction. The total heat transfer resistance is the effective thermal conductivity k, which accounts for all the mechanisms of heat transfer. The heat transfer rate is then calculated using the following equation:

$$\dot{Q} = -kA\frac{dT}{dx}$$

where Q is the rate of heat transfer (W), k is the thermal conductivity [W/(m·K)], A is the area perpendicular to the x direction (m2), and T is temperature (K).

3.4.5 Catalyst :

The reaction requires an acidic catalyst to assist the protonation of the carbonyl oxygen as it enhance the electrophilicity at the carbonyl carbon. Protonated carbonyl oxygen reacts quicker with any nucleophile in the solution, which is glycerol in this case. The acidic catalyst also lower the pH of the solution, which facilitates the elimination process of hydroxide group.

Amberlyst -15 is used as the acidic catalyst for the reaction. The catalyst has the advantage of being easy and safe to use. The catalyst has macro reticular polystyrene based ion exchange resin with strongly acidic sulfonic group so it serves as excellent source of acidic cation. Amberlyst-15 resin is widely used in esterification process.

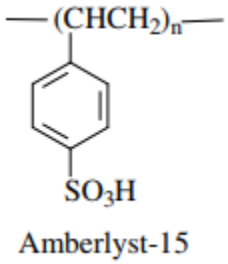

Amberlyst-15

Figure 3-1 :Structure of Amberlyst-15 [15]

3.5 Reaction kinetics

The kinetics of transacetalization of glycerol with 1,1-diethoxyethane in ethanol over Amberlyst-15 has been investigated at the temperature range 25 -40 C in Hong el al [3]. The study proposed a second-order kinetic model for the reversible reaction:

$$-\frac{dC_{DEE}}{dt} = \eta k W_C \left(C_{DEE} C_{Glycerol} - \frac{1}{K_C} C_{EtOH}^2 C_{Acetal} \right)$$

where η is the intraparticle effectiveness factor, k is the forward reaction rate constant per mass of catalyst, and WC is the mass of catalyst per unit volume of solution.

The incoming feed solution will have a large impact on the reaction. The study suggests using diethoxyethane as limiting reactant. Excessive diethoxyethane improves the conversion but also facilitates the unwanted side-reaction. Ethanol is added into the feed solution to serve as solvent, make the solution become one phase and allow for high initial reaction rate. The solution then become homogeneous. Ethanol is a product of the reaction so the process will modify the equilibrium to the reversible direction. However, the advantage of having a homogenous phase outweighs the disadvantage. The addition of ethanol into the initial feed is supported by laboratory result as the conversion of glycerol increases by more than 100%: from 35% to 80% [3]. Experiment is conducted for four feed solution with different mix ratio of glycerol, diethoxyethane and ethanol respectively to be : 1.5:1:4, 1:1:4, 1:1:8 and 1:1:12. The result is shown in figure 3-2

Reactant molar ratio	Measured equilibrium conversion			
	Glycerol		DEE	
Glycerol:DEE:EtOH	25 °C	40 °C	25 °C	40 °C
1.5:1:4	62.3%	64.3%	93.0%	89.2%
1:1:4	81.1%	78.6%	83.8%	81.5%
1:1:8	77.1%	75.2%	77.2%	73.4%
1:1:12	67.9%	65.1%	69.5%	62.4%

Figure 3-2: Conversion vs reactant molar ratio [12]

The reaction expresses best conversion at the molar ratio of 1.5:1:4 for glycerol :DEE:EtOH. However, the molar ratio of 1:1:12 is chosen because excess of ethanol is necessary to create a homogenous phase environment, improving the reaction rate. At other molar ratio, the reaction achieves higher conversion but it is canceled out by low reaction rate, making 1:1:12 be the most feasible choice for industrial purpose.

The study reports heat of reaction at -20.65 kJ/mol, an activation energy of 58.6kJ/mol and pre-exponential factor of ko = 7.85 10^5 m^6 /kmol/kg cat/s [3]. The Arrhenius equation relates temperature to reaction constant:

$$r_a = k_0 exp\left(\frac{-E}{RT}\right)$$

E represents the activation energy, T represents the reaction temperature, ko represents the pre-exponential factor, R represents the universal gas constant, and r_a represents the reaction rate constant.

The equilibrium constant is calculated by the Van-Hoff equation. The result is shown in the figure 3-2.

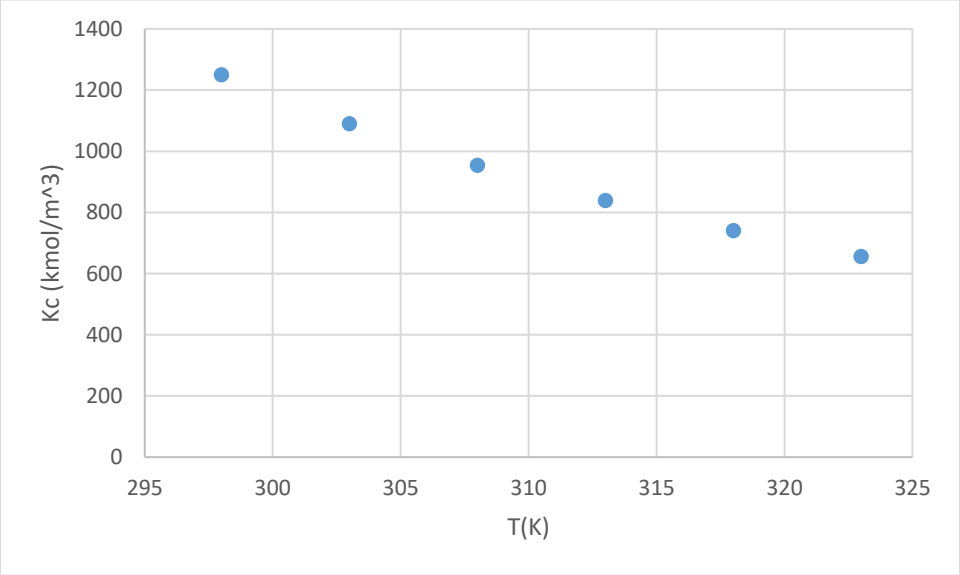

Figure 3-2: Equilibrium constant vs temperature

The equilibrium constant reduces as temperature increases, proving that the reaction is exothermic. It is still advisable to set the temperature as high as possible due to superior reaction rate. However, the highest temperature available is 40 C before side-reaction takes place and affects the purity of the product.

3.6 Computational Fluid Dynamics (CFD)

3.6.1 Introduction to CFD

Navier-Stokes or Euler equation provides methods to describe the motion of fluid but the challenge lies in obtaining approximate solution for those equations. However, the detailed solution requires the amount of effort far beyond what numerical analysis can offer. Understanding of fluid motion had to be dependent on experiment alone, which is always

subjected to human error and is time-consuming. The arrival of Computational Fluid Dynamic (CFD) in the twentieth-century resolved the problem. Modern computer can solve for the solution by doing thousands of computational analysis at a short amount of time. With power of computer, scientist can bypass the human limit for exhausting task as computing.

In chemical engineering, CFD is used to analyze the flow in pipe or operational unit. The modelled flow can then be scaled-up or used as empirical model for industrial purpose. CFD allows engineer to quickly change physical parameter such as temperature, linear velocity or species concentration to assess the impact of the change. The method is superior compared to traditional approach of doing pilot experiment.

3.6.2 Finite element method.

CFD employs numerical method to modify continuum problem (unlimited amount of degree of freedom) to discrete problem (finite amount of degree of freedom). To accomplish the task, CFD uses a process called discretization, which involves two steps. Step one is to divide the fluid domain into smaller subdomain named element. The density of element varies based on preference of the engineer. The density can be made finer in the area that accuracy is the top priority while made coarse in less important area. Step 2 is to convert the governing equation into the form that can be used in each element. There are many ways to run the discretization method but the study will employ finite element method.

In this method, the domain is divided into a number of subdomains. The higher the number of domain, the more accurate is the solution. Solution for each subdomain is computed and then it is connected to each other to compute a final solution. The connecting point between each element is named node and the compendium of subdomain is called mesh. This way, a complex partial differential equation (PDE) can be broken down into many more simplified PDE.

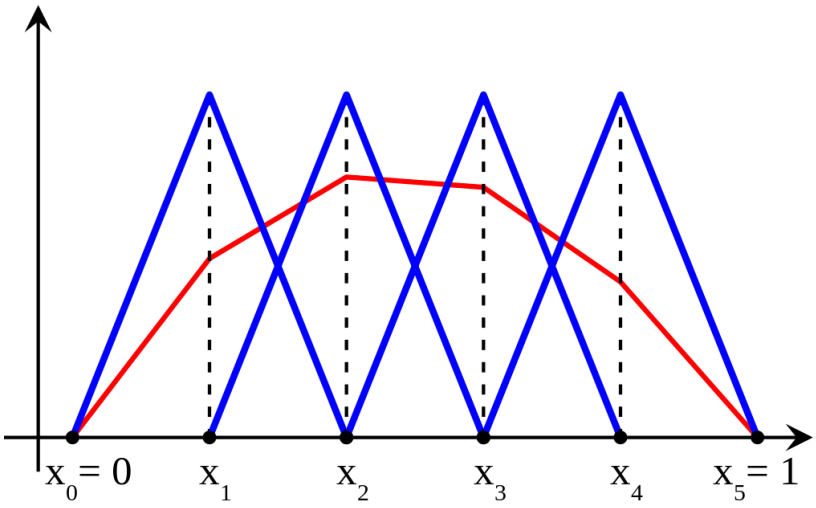

Figure 3-4 : Finite element method [17]

3.6.3 COMSOL Multiphysics

COMSOL is a powerful mathematic solver that is based on the finite element method. COMSOL allows user to modify the mesh structure at will. COMSOL is a multiphysics software, meaning it can couple two or more physical phenomenon into its solution. This feature is important as most real world problem involve more than one physical phenomena. COMSOL has built in common physical equations so it reduce the effort of scientist of having to build complicated equation. COMSOL is an application of CFD so engineer can do the "what if" study by changing physical parameter easily through COMSOL interface. As such, COMSOL is suitable as mathematical program for the study.

4. Methodology

4.1 Process Overview

The fixed bed reactor is modelled using COMSOL Multiphysics 5.2. The software employs finite element method to solve PDE/ ODE that appear in the model. The model will demonstrate the concentration profile of all compound as it varies along the axis of the reactor. Other physical parameter profile such as temperature and pressure are also computed. The fixed bed reactor is modelled as 1 D+1D. The reactor is considered to be an one dimensional tube as shown in Figure 4-1.There are spherical catalyst pellet on each point along the one dimensional tube. The catalyst pellet is represented by two-dimensional square in COMSOL but transport phenomena

will only occur on the y-axis so it is essentially an one-dimensional model. Combining the two model will allow COMSOL to compute physical profile in the reactor accurately.

Figure 4-1 Reactor model

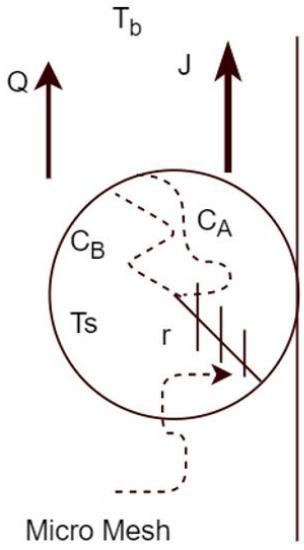

Figure 4-2 Spherical pellet model

Each model (Reactor and catalyst pellet) involves two different mode : Transport of Diluted Species and Heat transfer physics. Transport of Diluted Species is responsible for the chemical reaction and mass transfer process in both model. In reactor model, Heat transfer in Liquid

mode was used while Heat transfer in Solid mode was implemented for pellet model.Each mode will provide its own governing PDE/ODE so COMSOL can solve using FEM.

4.2 Mass transfer

The mass transfer process inside the reactor and catalyst pellet is described by Transport of Diluted Species mode. For the reactor, the governing equation represents the diffusion in bulk fluid flow is :

$$\frac{1}{A_C}\frac{dF_i}{dz} - a_p(1-\varepsilon_b)k_g(c_{pi}^s - c_i) = D_{ea}\frac{d^2C_i}{dz^2}$$

where Ac represents the cross-sectional area of the reactor tube (m2), Fi represents the molar flow rate of component i (mol/s), ap represents the ratio of the pellet's surface area to volume (m-1), $\varepsilon b$is the bed void fraction, kg is the particle-to-fluid mass transfer coefficient (m/s), c^{s}_{pi} is the concentration of component i at the pellet domain's surface (mol/m3), Ci is the concentration of component i in the reactor domain (mol/m3), and Dea is the reactor's axial dispersion coefficient (m2 /s).

The stream coming in is considered radially well-mixed so the concentration of any compound is constant over the reactor's cross section. There is only diffusion along the axis of the reactor. Convection mass transfer is also considered in the model.

The following equation represents diffusion in catalyst pellet:

$$\frac{1}{r^{*2}}\frac{d}{dr^*}\left(D_{ip}r^{*2}\frac{dC_{pi}}{dr^*}\right) = -\sum_{j=1}^{NR}\alpha_{ij}r_j$$

where , $r*$ represents the radial position within the pellet (m), D_{ip} represents the diffusivity of component i in the pellet (m2 /s), C_{pi} represents the concentration of component i in the pellet (mol/m3), α_{ij} represents the stoichiometric coefficient of component i in reaction j, and rj represents the rate of reaction j (mol/m3 s). To simplify the computing process, diffusion only exist over cross section of the pellet. Chemical reaction is coupled with the diffusion process inside the pellet.

4.3 Heat transfer

The following equation is employed to compute the temperature profile inside the reactor:

$$\frac{2\alpha_L}{R}q_w + \frac{k_{ea}}{\alpha_L}\frac{d^2T_f}{dx^2} + \alpha_L a_p(1-\varepsilon)h_g\left(T_s^s - T_f\right) = \rho\hat{C}_{pf}u\frac{dT_f}{dx}$$

Where q_w represents the wall heat flux (W/m2), k_{ea} represents the axial thermal dispersion coefficient (W/m.K), hg represents the particle-fluid heat transfer coefficient (W/m2K), $Ts\ s$ represents the catalyst temperature at its surface (K), T_f represents the fluid temperature (K), $\hat{C}_{pf}$ represents the fluid heat capacity (J/kg.K), and u represents the linear fluid velocity (m/s).

Similarly, in the catalyst pellet domain:

$$0 = \frac{d}{dy}\left(k_p\frac{dT_s}{dy}\right) + \left[\alpha^2\sum_i \rho_s(-\Delta H_{r,i})r_i + \frac{2}{y}k_p\frac{dT_s}{dy}\right]$$

Where kp represents the thermal conductivity of the catalyst pellet (W/m.K), T_s represents the temperature of the catalyst sphere (K), and ΔH_r, represents the enthalpy of the reaction (J/mol).

The main heat transfer mechanism is conduction which is governed by Fourier's law. As the chemical reaction is an exothermic reaction, the temperature is expected to increase along the reactor.

4.4 Pressure Drop

Ergun equation represents the pressure drop across the reactor:

$$\frac{dP}{dz} = -\frac{(1-\varepsilon_b)G}{d_p\varepsilon_b^3\rho_{feed}}\left[150\frac{(1-\varepsilon_b)\mu_f}{d_p} + 1.75G\right]\frac{\rho_{feed}}{\rho}$$

where P represents pressure (Pa), z represents the axial coordinate of the reactor (m), εb represents the average bed voidage ($volume\ of\ reactor - volume\ of\ catalyst\ particles$)/ $volume\ of\ reactor$), G represents the mass flux (kg/m2 s), dp represents the catalyst pellet diameter (m), μf represents the fluid viscosity (kg/m s), and ρ is the fluid density (kg/m3). The

bed voidage, εb, was provided by de Klerk [17], who calculated average bed voidages for various particle-to-column ratios of tubular columns packed with spherical catalysts.

The PDE of Ergun equation is entered in a different module manually. The boundary condition of the reactor outlet is atmospheric pressure to be suitable for industrial purpose.

4.5 Physical property

The governing equations for each module require physical parameter input. Several physical relationships are used to determine these necessary properties.

4.5.1 Viscosity

Viscosity of multicomponent ideal mixture in liquid phase is calculated using Papaioannou correlation[18].

$$\ln \eta^{ID} = \sum_i x_i \ln \eta_i$$

Where η^{ID} is the viscosity of multicomponent ideal mixture in liquid phase, x_i is the mass fraction of each component and η_l is the viscosity of each correspond component.

4.5.2 Axial Dispersion

Edwards and Richardson provides correlation to compute axial dispersion[19]:

$$\frac{1}{Pe} = \frac{0.73\varepsilon}{Re \cdot Sc} + \frac{0.5}{1+\frac{9.7\varepsilon}{Re \cdot Sc}}$$

$$D_{ea} = \frac{u \cdot d_p}{Pe}$$

Where ε is the bed void fraction, Re is the Reynolds number, Sc is the Schmidt number, u is the linear fluid velocity (m/s), dp is the pellet diameter (m) and Dea is the axial dispersion coefficient (m2 /s).

4.5.3 Particle fluid mass transfer coefficient

The particle-fluid mass transfer coefficient was obtained from the following correlation from Wakao and Funazkri [20]:

$$Sh = 2 + 1.1Re^{0.6}Sc^{1/3}$$

$$k_g = \frac{Sh \cdot D_{AB}}{d_p}$$

Where D_{AB} is the average binary diffusivity within the particle (m2 /s) and kg is the particle-fluid mass transfer coefficient (m/s).

4.5.4 Diffusion Coefficient.

Two different diffusion coefficient is calculated for two different diffusion process in the model : diffusion in the bulk flow and diffusion inside the catalyst pellet. Diffusion inside the bulk flow occurs as a result of the difference in concentration across the reactor. The diffusion process is characterized by mass transfer coefficient k_C that obtained from Sherwood correlation and diffusitivity D_{AB} acquired from Wilke- Chang correlation.

Diffusion in catalyst pellet is not only affected by Fick's law but also the porous characteristic of the pellet. As fluid has to travel through catalyst pore to get inside the pellet, the surface area reduces. Inside the pellet, the fluid also has to travel in a curve line instead of a straight line due to the tortuous nature of the pore. Porosity and tortuosity is multiplied into the Fick's law to account for this effect.

4.6 Chemical reaction

The reversible kinetic equation for transacetalization of glycerol is proposed by Hong et al [3]:

$$-\frac{dC_{DEE}}{dt} = \eta k W_C \left(C_{DEE} C_{Glycerol} - \frac{1}{K_C} C_{EtOH}^2 C_{Acetal} \right)$$

where η is the intraparticle effectiveness factor, k is the forward reaction rate constant per mass of catalyst, and Wc is the mass of catalyst per unit volume of solution.

The forward reaction rate constant is calculated by Arrhenius equation with pre-exponential of 7.85 10^5 m6 /kmol/kg cat/s. Kc is observed to be 1250 kmol/m^3 at 20 C. Kc at other temperature is extrapolated using Van-Hoff equation :

$$\ln \frac{K_2}{K_1} = \frac{-\Delta H^{\ominus}}{R} \left(\frac{1}{T_2} - \frac{1}{T_1} \right)$$

where K_{eq} is equilibrium constant, ΔH is heat of reaction, calculated to be -20.5kJ/mol [3]. R is gas consant and T is temperature in K.

The intraparticle effectiveness factor is calculated using observable modulus:

$$F=\eta \phi^2$$

With F is the observable modulus, η is the intraparticle effectiveness factor and ϕ is the Thiele modulus. The Thiele modulus is extrapolated from the plot of η vs Thiele modulus provided by Smith[3].

4.7 Operating condition

The composition of the fluid coming in is 1:1:12 for Glycerol:DEE: Ethanol by molar fraction. The reactor radius, length, temperature, flow rate is varied for optimization. The outlet pressure is set at 1 atm while COMSOL will compute inlet pressure based on pressure drop across the reactor.

Hong et al[3] suggests temperature should not be over 50 C to avoid side reaction so temperature will be monitored to be lower than 50 C. As the reaction is in liquid phase, pressure has little effect on the overall process but pressure drop is concerned due to economic reason. Other parameter such as reactor radius, length or flow rate are expected to affect the conversion rate.

5. Results and discussion

5.1 Operating temperature

Operating temperature affects maximum conversion rate. The reaction is exothermic so high temperature will reduce maximum conversion. **Figure 5-1** confirms the theory as maximum conversion slightly reduces when operating temperature increases.

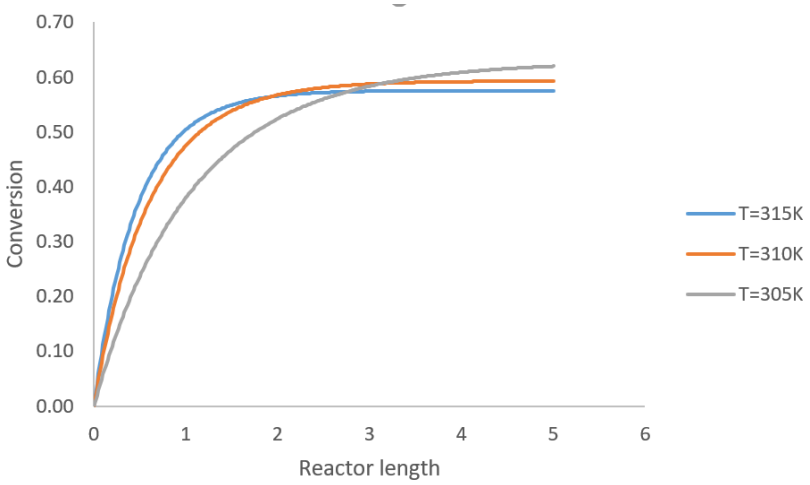

Figure 5-1: Temperature vs Maximum conversion

Figure 5-2 shows that increasing temperature will increase reaction rate. However, Hong et al [22] suggests that it is important for the temperature to be below or equal to 50 C so side reaction does not occur. While 50 C is the optimal temperature, the actual maximum operating temperature is 45 C to account for the heat generated from the reaction. Since the reactor is adiabatic, no cooling system will be applied to mitigate the effect of increasing temperature. **Figure 5-3** shows that with a feed temperature of 45 C, the maximum temperature of the reactor is 49 C, satisfying the condition.

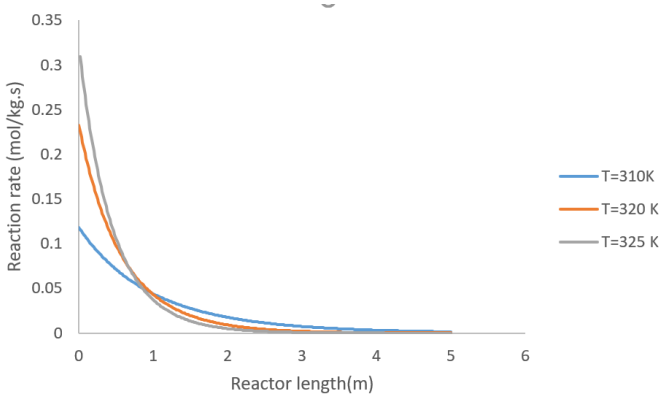

Figure 5-2: Reaction rate vs Temperature

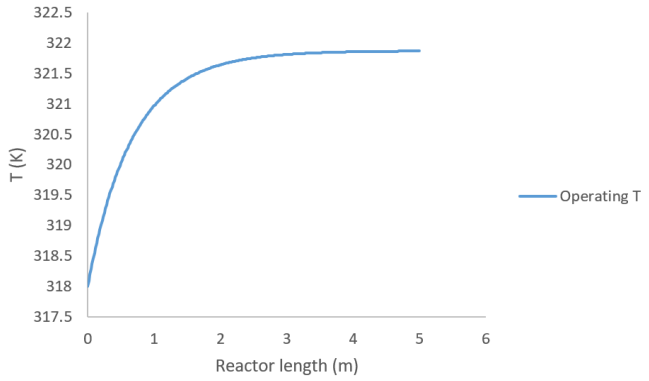

Figure 5-3: Maximum temperature

Diffusion rate increases with temperature but effectiveness factor reduces (**Figure 5-4**). Elevating temperature increases both reaction rate and diffusion rate but reaction rate increases faster than diffusion rate.

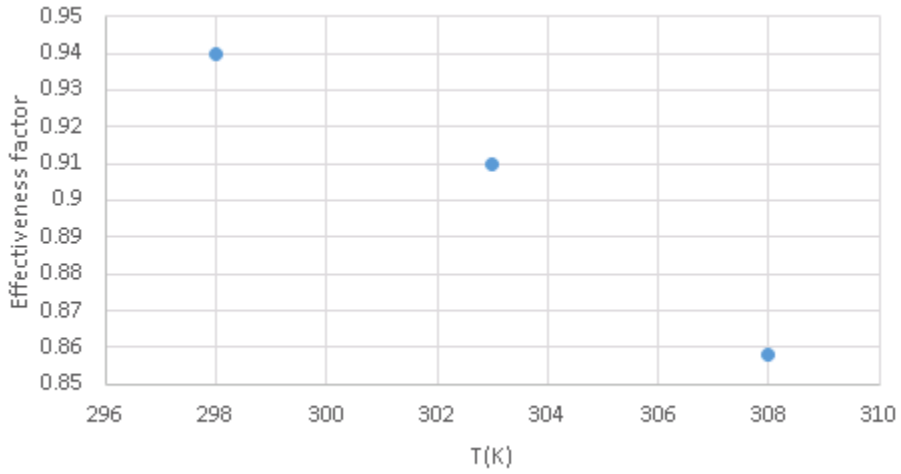

Figure 5-4:Effectiveness factor vs temperature

Figure 5-5 shows how conversion change when operating temperature is increased. In general, at the same reactor length, conversion increases substantially when operating temperature increases.

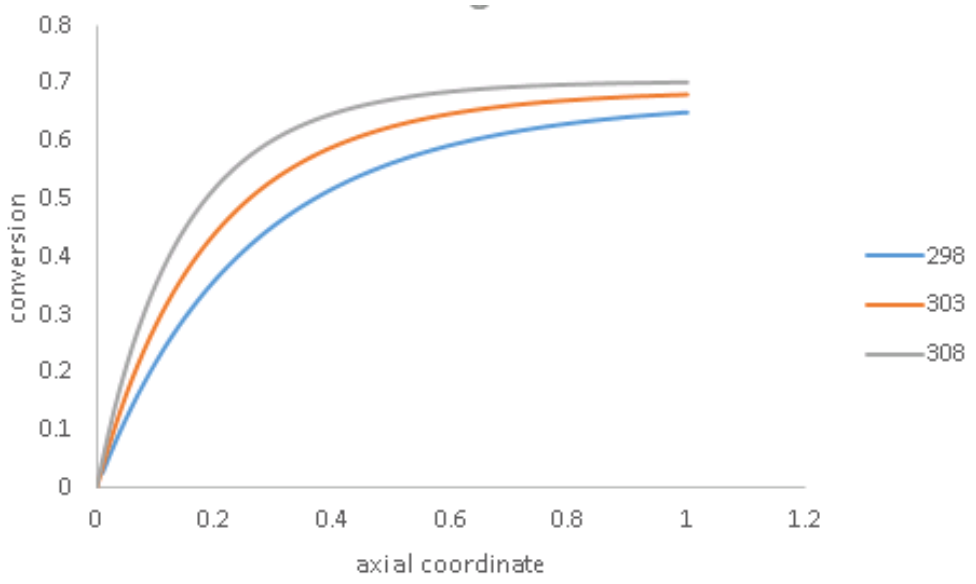

Figure 5-5: Temperature vs conversion

5.2 Pressure

Figure 5-6 shows how operating pressure affects the reaction rate. As expected, reaction rate is unaffected by pressure since the reaction occurs in liquid phase. Reaction rate curve at P= 4 atm, P = 5atm and P = 6 atm are on top of each other.

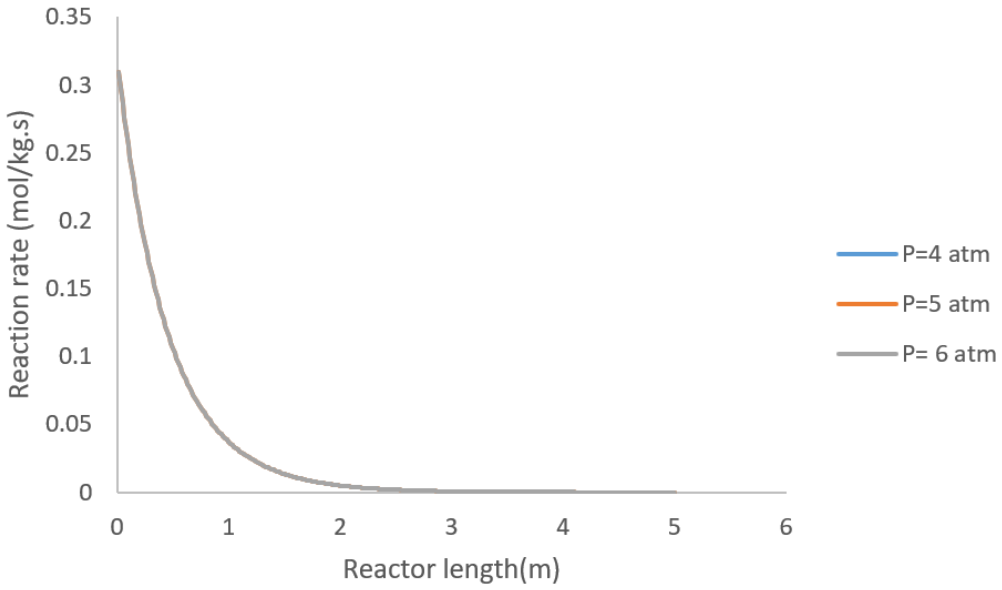

Figure 5-6 :Pressure vs Reaction rate

Figure 5-7 shows the relationship between pressure and effectiveness factor. Effectiveness factor is observed to be stable even with the increase of pressure. Diffusion rate is unaffected by pressure in liquid phase since liquid is incompressible. On top of that, reaction rate is also independent of pressure in liquid phase unlike gas phase, where a change in pressure may alter the total concentration of component in the mixture. Pressure drop is unavoidable in any reactor so the fact that pressure drop may not have any noticeable effect on the reaction is beneficial. The chemical process is assured to maintain consistency across the reactor, which a reaction in gas phase cannot offer.

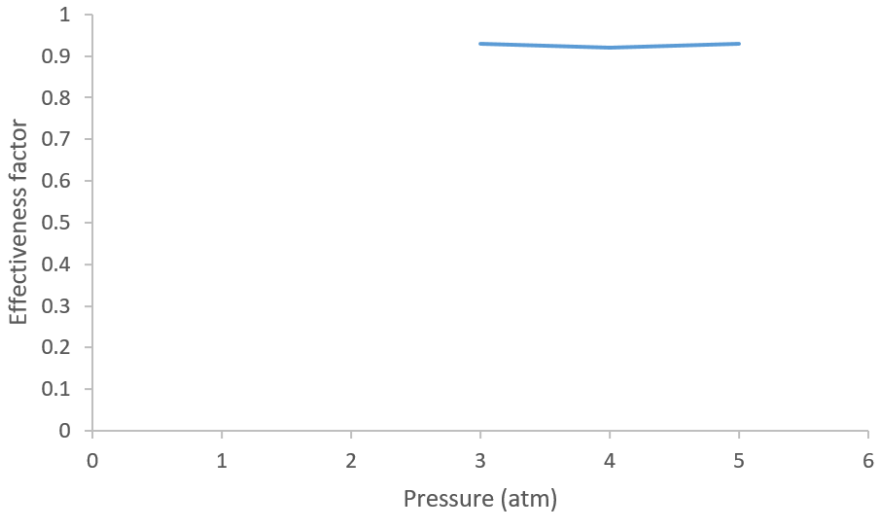

Figure 5-7:Pressure vs Effectiveness factor

For the reasons above, it is no surprise when pressure does not affect conversion rate, as demonstrated in **Figure 5-8**. Engineer is free to choose any value for pressure that is economical.

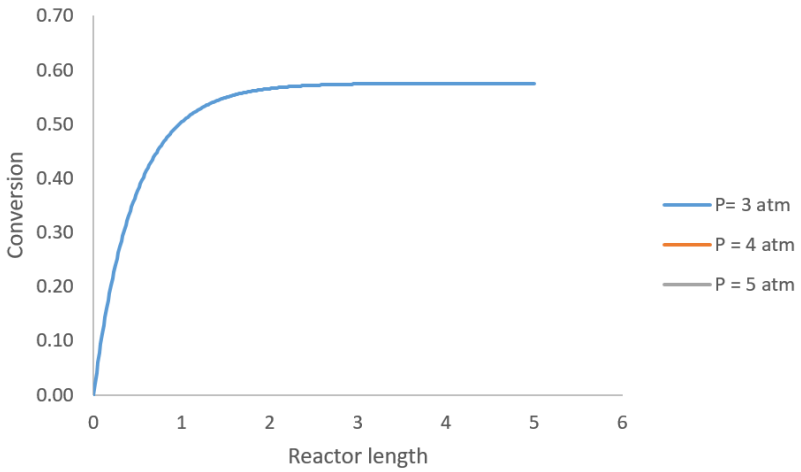

Figure 5-8 : Pressure vs conversion

5.3 Flow rate

Figure 5-9 shows that high flow rate has positive impact on reaction rate as more reactants are poured into the system. The consumption rate is also increased as the reactor can always maintain high concentration of reactant. High flow rate also improves mass transfer rate and therefore increases effectiveness factor, as demonstrated in **Figure 5-10.** However, the downside is low residence time. Before the reaction occurs, reactants already flow out of the reactor. **Figure 5-11** shows the decisive impact of this downside as conversion is lower even though reaction rate increases. This phenomenon might come into consideration for design recommendation.

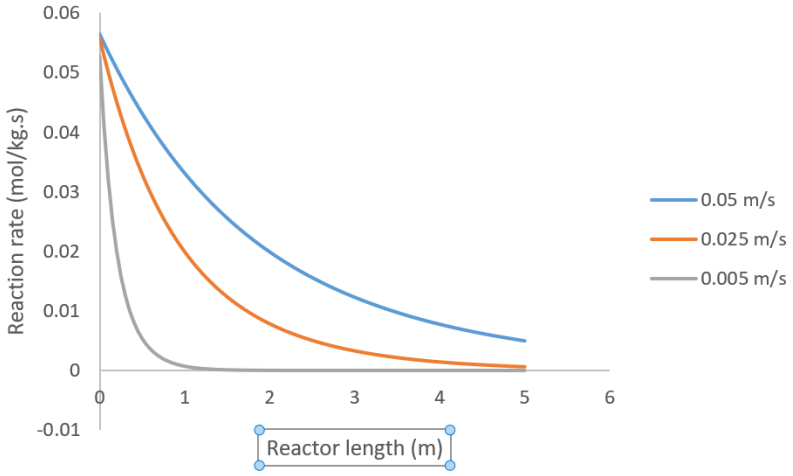

Figure 5-9: Flow rate vs reaction rate

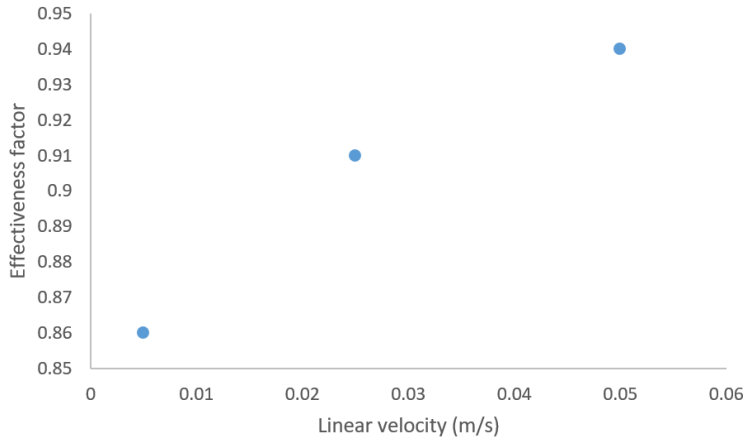

Figure 5-10: Linear velocity vs effectiveness factor

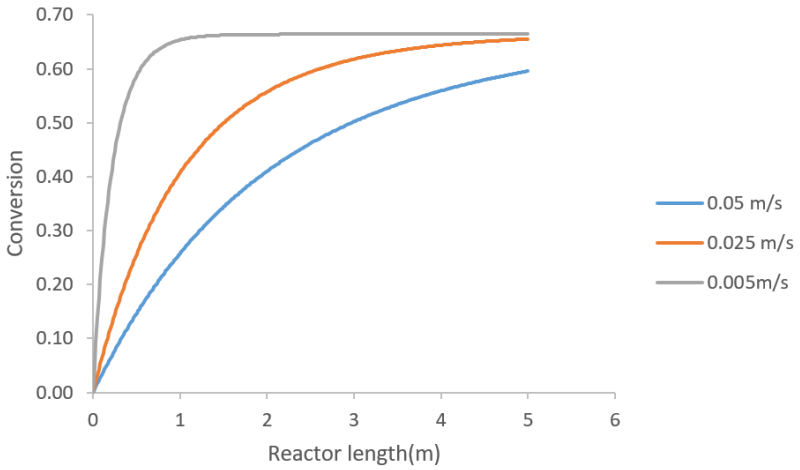

Figure 5-11: Flow rate vs conversion

Flow rate also affects pressure drop along the reactor. Since liquid is incompressible, pressure drop only occurs as a form of head loss. From examining Ergun Equation, it can be inferred that pressure drop will increase when flow rate increases. While pressure has no substantial effect on conversion, it is desirable to have low pressure drop for economic reason suchs as reducing pump or compressor cost. **Figure 5-12** show the pressure profile along the reactor when flow rate is varied. Pressure drop is proved to be neglectable.

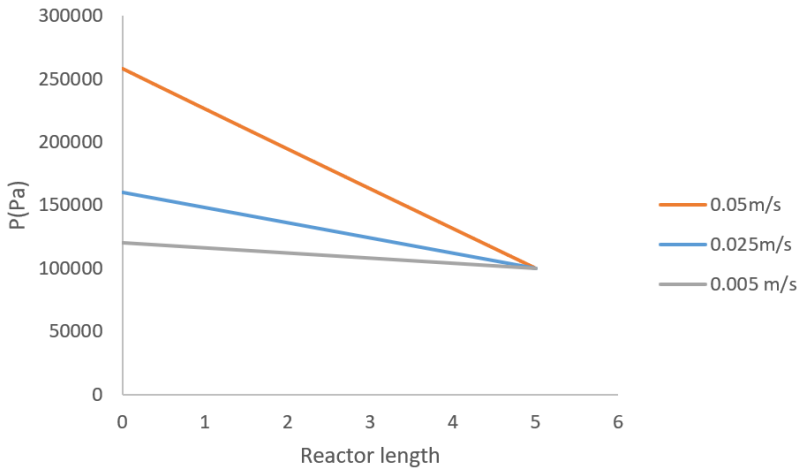

Figure 5-12: Pressure vs flow rate

5.4 Catalyst pellet

The reaction uses Amberlyst-15 as acidic catalyst for the reaction. Amberlyst -15 can be acquired in different form or particle diameter so the selection of catalyst is important.

As the purpose of the simulation is to model fixed bed reactor, solid form of Amberlyst-15 is selected. **Figure 5-13** show the effect of pellet diameter on effectiveness factor. Large catalyst pellet reduces the ability of reactants to penetrate into interior of the pellet, keeps the production rate of the pellet low.

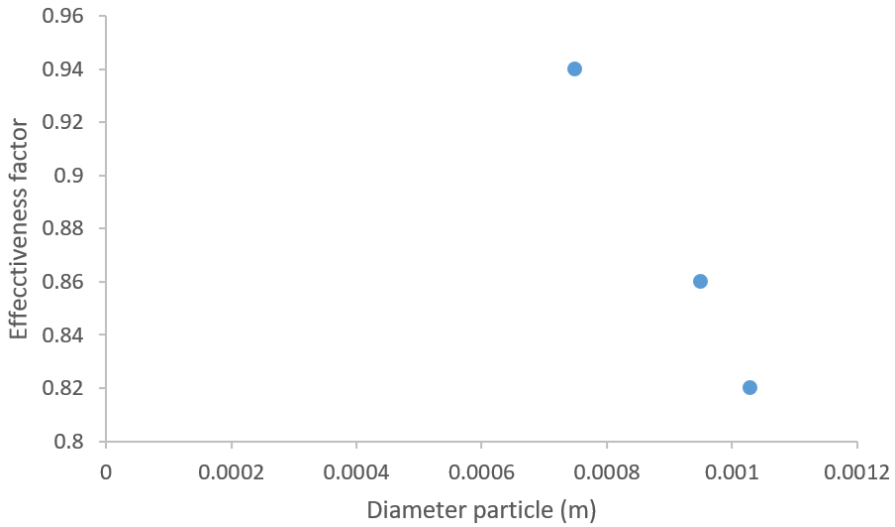

Figure 5-13: Effectiveness factor vs Diameter particle

As diameter of catalyst pellet changes, the ratio of reactor to catalyst pellet radius also changes, which changes the bed voidage. De Klerk'study provides the estimation of bed voidage based on reactor to catalyst pellet radius ratio[17]. Low bed voidage indicates good packing quality so high reactor radius to pellet ratio is desirable.

$R_r : r_p$ ratio	Bed Voidage
4.2	0.425
4.9	0.419
7.2	0.397
9.2	0.368
11.2	0.366

Table 5-1 : . Reactor-to-Catalyst-Pellet Radius Ratio and Corresponding Bed Voidage [17]

Assume reactor radius is kept constant, **Table 5-1** shows the conversion rate when catalyst pellet diameter is varied. The conversion rate is higher at as pellet diameter gets smaller. This observation is consistent with theory since the effectiveness factor is maximized. It should be noted that with such high reactor radius to pellet ratio, any attempt to cool or heat the reactor is futile. However, since the reactor is considered adiabatic, this is a minor problem. The feed temperature plays a more important role in deciding operating temperature.

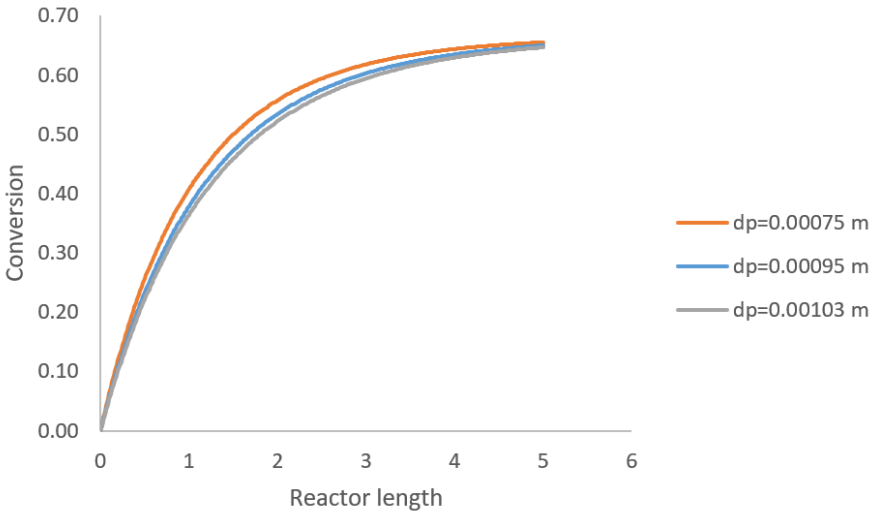

Figure 5-14: Conversion vs reactor length

Catalyst pellet diameter directly affects pressure drop, as shown in **Figure 5-15.** The pressure drop is minimal and does not require huge cost for compressor/pump.

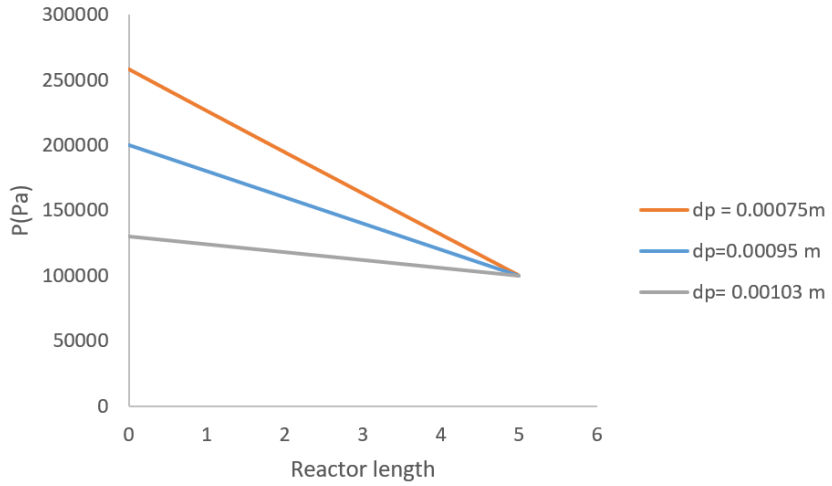

Figure 5-15: Pressure drop vs pellet diameter

5.5 Reactor Design

5.5.1 Reactor Radius

Figure 5-16 shows how conversion rate varies with radius of the reactor at constant flow rate. Conversion rate is higher as reactor radius increases. Big reactor radius results in low linear velocity for the same flow rate and therefore increases residence time. Another reason behind this phenomenon is the increase in reactor radius to pellet ratio which improves bed voidage.

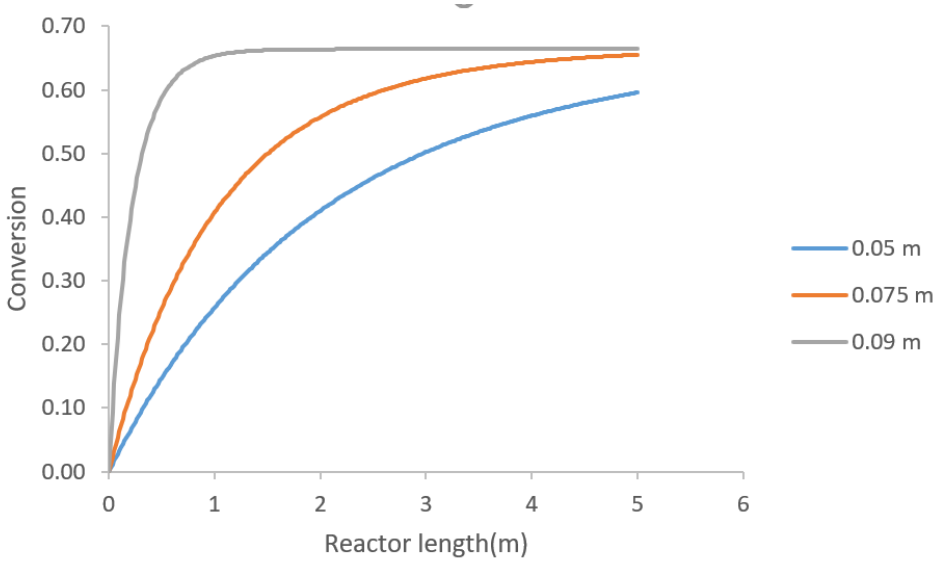

Figure 5-16: Conversion vs reactor diameter

5.5.2 Reactor length.

The effect of reactor length on conversion is demonstrated in **Figure 5-17**. Generally, longer reactor allows larger residence time and therefore increasing conversion rate. However, since the reaction is reversible, there is a limit on the achievable rate of conversion. Even with infinite reactor length, conversion may not go over 60%.

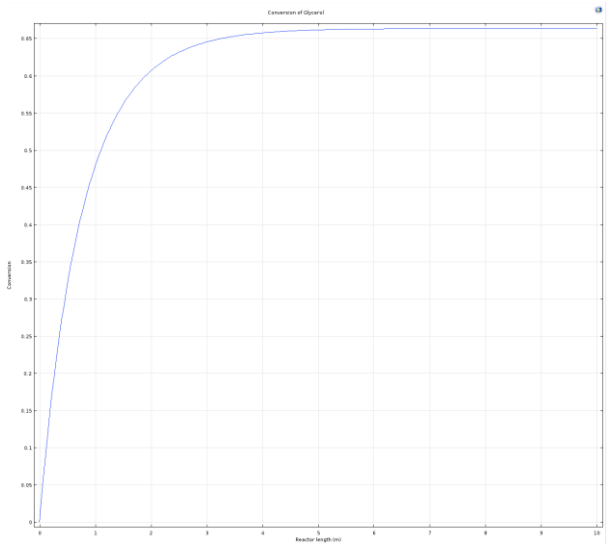

Figure 5-17: Conversion of Glycerol vs reactor length.

6. Recommendation

6.1 Operating Temperature

High temperature exhibits positive effect on conversion rate but negative effect maximum conversion as the reaction is endothermic. . Hong et al[?] shows that temperature should be set below 50 C to avoid side-reaction. Therefore, the operating temperature is recommended to be 48 C. The reactor is considered adiabatic so the feed temperature is the same as operating temperature

6.2 Operating Pressure

Pressure has no effect on the process as the reaction progresses in liquid phase. However, it is desirable to have a pressure outlet of 1 atm. Pressure drop varies with reactor length and linear velocity but even in the most extreme condition, pressure drop does not exceed 5 atm.

Engineer can choose any operating pressure for the process without concern about reducing efficiency of the reactor.

6.3 Reactor length

Conversion and purity of the product are both increased with reactor length. While it is recommended to have long reactor to achieve maximum conversion, the trade-off for economic is the downside. Further research on this trade-off relationship is required to make better assessment on the length of the reactor.

6.4 Reactor radius.

Large radius reduces linear velocity, which in turn increase residence time at the same flow rate. Large residence time allows more reactants to react and therefore increase conversion rate per meter tube length of reactor. In other word, large radius effectively reduces the reactor length. Other quantitative research on this topic have to be done before a conclusion was made.

6.5 Flow rate

At the same radius, large flow rate leads to high consumption rate because the feed replenish the reactant concentration with higher rate. High consumption rate produces more product but reduces the efficiency of the reactor. In details, the conversion rate is slowing down when larger flow rate was set at the same reactor's radius.

7. Conclusion

Transactelization of glycerol has emerged as a solution to the redundance of biodiesel by-product. The reaction converts glycerol into gycerol acetal, which can act as fuel additive for a variety of reactions. The report examines the feasibility of using transactelization of glycerol as a method of utilizing biodiesel by-product by simulating the reaction in a heterogeneous model in COMSOL. The model is built as a one-dimensional fixed bed reactor and solved by Finite Element Method. Mass transfer, pressure drop, heat transfer and chemical reaction are all considered by the model. Upon resolving, the model will compute the profile of temperature, pressure and concentration at each point along the reactor, allowing determining the feasibility of the reaction in a fixed bed reactor.

The result confirms the success of the transactelization of glycerol in fixed bed reactor. Potential concern includes the composition of the feed coming in, which might be uneconomical. The feed ratio is chosen to minimize the impact of diffusion limitation but the cost is likely to rise high due to difficulties in treating biodiesel-by product to produce the required feed composition. Simulation with different feed composition is strongly encouraged to further reduce the cost. This study disregards the side-reaction of converting to undesired isomer of glycerol acetate but future study might want to consider the effect of side-reaction.

To optimize the reactor for transactelization of glycerol, various physical parameters are tuned. High operating temperature is essential to increase the conversion and the recommendation is to not raise the temperature over 45 C before risking major side-reaction. Operating pressure is not important in liquid-phase reaction, but it is desirable to adjust the outlet pressure to atmospheric pressure. Pressure drop inside the reactor is neglectable and does not have harmful effect on the chemical process. Effectiveness factor is reasonably high so pellet size is ultimately not important for the range of pellet diameter tested in the study. The main design parameter is the flow rate, length and radius of the reactor as they affect conversion and production rate.

8. Reference

[1] Franclemont, Joshua, and Selma M. Thagard. Electrical Discharges Directly in Liquid Glycerol for the Production of Hydrogen, IEEE, 2013, doi:10.1109/PLASMA.2013.6633201.

[2]Ferreira, M. O., et al. "Glycerol as Additive for Fuels - a Review." *LATIN AMERICAN APPLIED RESEARCH* 44.1 (2014): 47. Print.

[3]Hong, Xi, et al. "Reaction Kinetics of Glycerol Acetal Formation Via Transacetalization with 1,1-Diethoxyethane." *Chemical Engineering Journal* 222 (2013): 374-81. Print.

[4]"EPA Comments on Biodiesel Decision." *Pro Farmer* 45.47 (2017): 1. Print.

[5]Perona, John J. "Biodiesel for the 21st Century Renewable Energy Economy." *Energy Law Journal* 38.1 (2017): 165. Print.

[6]Marchetti, Jorge Mario, and Ebook Central - Academic Complete. *Biodiesel Production Technologies*. New York: Nova Science Publishers, 2010. Web.

[7]Likozar, B., A. Pohar, and J. Levec. "Transesterification of Oil to Biodiesel in a Continuous Tubular Reactor with Static Mixers: Modelling Reaction Kinetics, Mass Transfer, Scale-Up and Optimization Considering Fatty Acid Composition." *Fuel Processing Technology* 142 (2016): 326-36. Print.

[8]Eda Çelik, St, et al. "Use of Biodiesel Byproduct Crude Glycerol as the Carbon Source for Fermentation Processes by Recombinant Pichia Pastoris." *Industrial and Engineering Chemistry Research* 47.9 (2008): 2985-90. Print.

[9]Yang, FX, MA Hanna, and RC Sun. "Value-Added Uses for Crude Glycerol-a Byproduct of Biodiesel Production." Biotechnology for Biofuels, vol. 5, no. 1, 2012, pp. 13-13.

[10]Wilkens, Erik, et al. "High-Level Production of 1,3-Propanediol from Crude Glycerol by Clostridium Butyricum AKR102a." Applied Microbiology and Biotechnology, vol. 93, no. 3, 2012, pp. 1057-1063.

[11]Wei, Lin, et al. "Co-Gasification of Hardwood Chips and Crude Glycerol in a Pilot Scale Downdraft Gasifier." Bioresource Technology, vol. 102, no. 10, 2011, pp. 6266-6272.

[12]Olm, Amanda Student author -- CM, MacDonald, Bryan Joseph Student author -- CM, and Dixon, Anthony G. Faculty advisor -- CM. Reaction and Transport in Industrial-Scale Packed Bed Steam Reforming of Glycerol. Worcester Polytechnic Institute, Worcester, MA, 2014.

[13]Walas, Stanley M., and Ebook Central Perpetual and DDA. Reaction Kinetics for Chemical Engineers. Butterworths, Stoneham, Massachusetts, 1989.

[14]Worstell, Jonathan, and Ebook Central Perpetual and DDA. Adiabatic Fixed-Bed Reactors: Practical Guides in Chemical Engineering. Butterworth-Heinemann, Waltham, Massachusetts, 2014.

[15]Pal, Rammohan, Taradas Sarkar, and Shampa Khasnobis. "ChemInform Abstract: Amberlyst-15 in Organic Synthesis." Cheminform, vol. 43, no. 43, 2012, pp. no-no.

[16de Klerk, A. Voidage Variation in Packed Beds at Small Column to Particle Diameter Ratio. American Institute of Chemical Engineers Journal, 49, 2003, 2022-2029.

[17]Papaloannou, Dimitri, Thomai Evangelou, and Constantinos Panayiotou. "Dynamic Viscosity of Multicomponent Liquid Mixtures." Journal of Chemical and Engineering Data, vol. 36, no. 1, 1991, pp. 43-46.

[18]Pepper, Darrell W., Juan C. Heinrich, and ENGnetBASE. The Finite Element Method: Basic Concepts and Applications with MATLAB, MAPLE, and COMSOL. CRC Press, Taylor & Francis Group, CRC Press is an imprint of the Taylor & Francis Group, an informa business, Boca Raton, 2017.

[19]Edwards, M. F., and J. F. Richardson. Gas Dispersion in Packed Beds. Chemical Engineering Science, 1968, 23.2, 109-23.

[20]Wakao, N., and T. Funazkri. Effect of Fluid Dispersion Coefficients on Particle-to-Fluid Mass Transfer Coefficients in Packed Beds. Chemical Engineering Science, 1978, 33.10, 1375-84.

9. Appendix

Appendix A: Viscosity model for liquid mixture

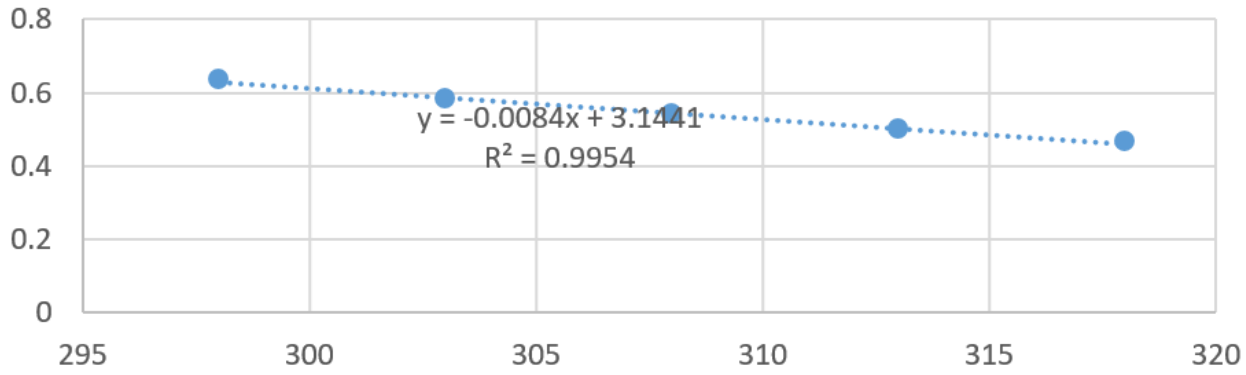

Appendix B: Thermal conductivity model for liquid mixture

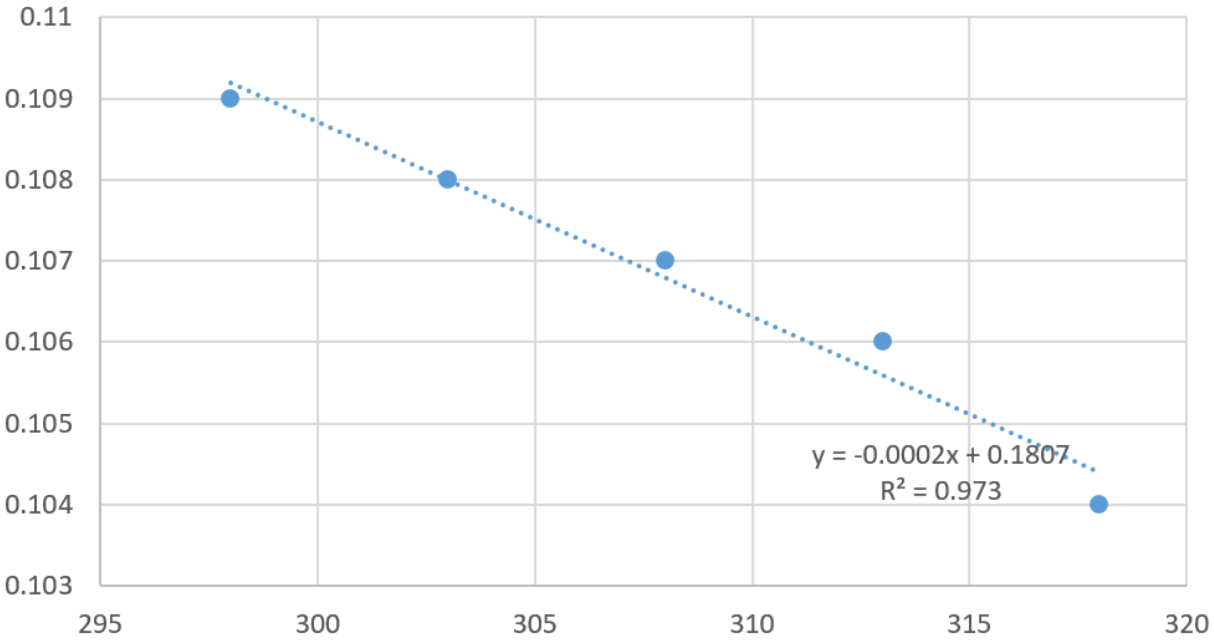

Appendix C: Heat capacity model for liquid mixture

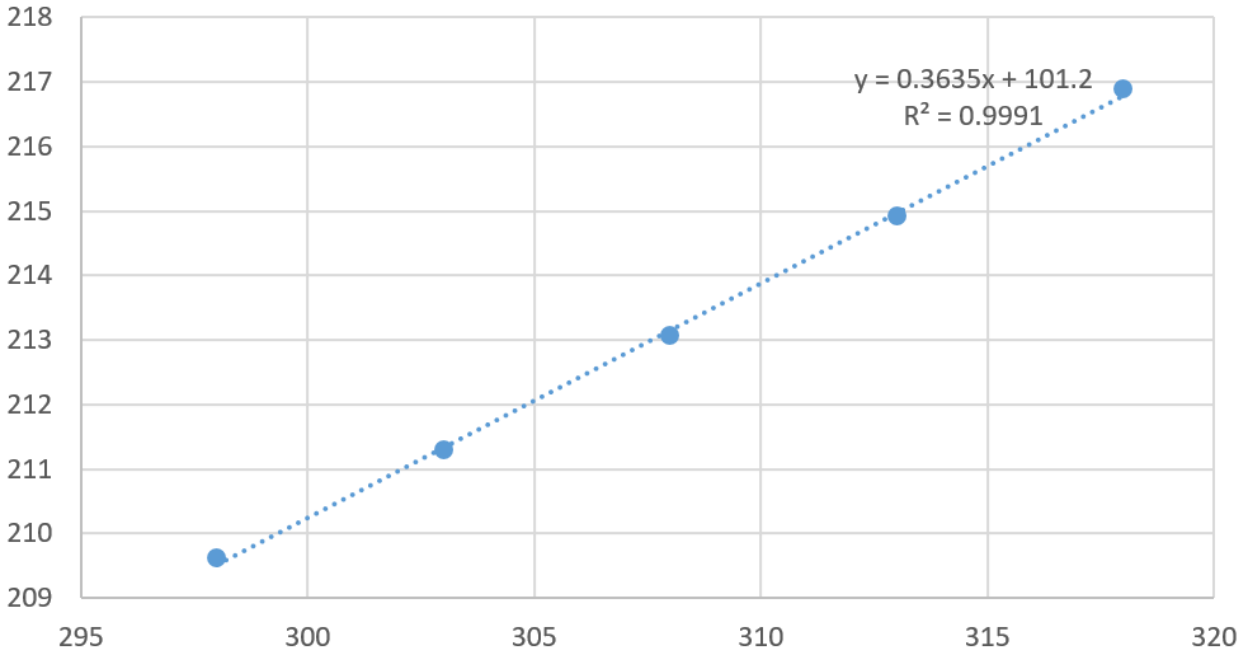

Appendix D: Effective diffusivity model for liquid mixture

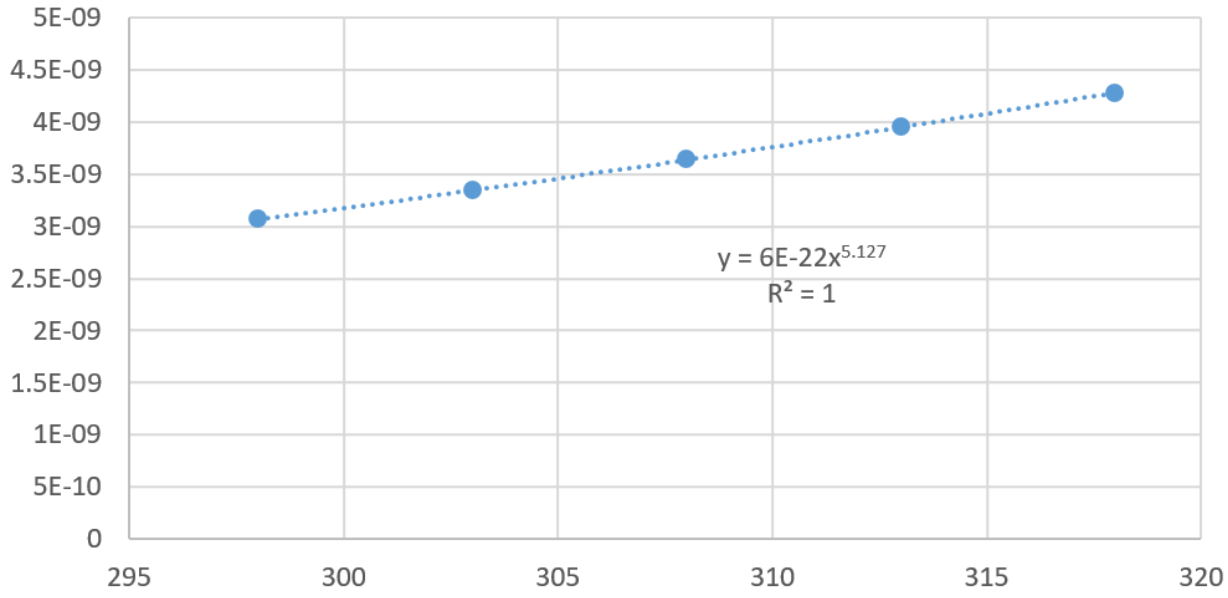

Appendix E: Simulation parameter

P_feed	3e5[Pa]	Feed pressure
T_feed	300[K]	Temperature
rho	842 [kg/m^3]	Inlet density
x_C3H8O3_feed	0.07	Molar fraction of C3H8O3 in feed
x_dee_feed	0.07	Molar fraction of def in feed
x_et_feed	1-x_C3H8O3_feed-x_dee_feed	Molar fraction of etOH in feed
F_gly	0.03[mol/s]	Molar glycerol feed rate
F_feed	F_gly/x_C3H8O3_feed	Feed molar flow rate
G	F_feed*MW_feed/Ra	Mass flux
u	G/rho	Inlet velocity
dt	0.05[m]	Reactor radius
dp	0.00105[m]	Particle diameter
N	dt/dp	Tube-to-particle diameter ratio
Ra	pi/4*dt^2	Reactor cross-sectional area
rp	dp/2.0	Pellet radius
Ap	3/rp	Surface area of particles per unit volume
scale	rp/1[m]	Pellet scale factor
L	10.0[m]	Tube length
scale_L	L/1[m]	Tube scale factor
kp	1[W/(m*K)]	Pellet thermal conductivity
rho_p	770[kg/m^3]	Density of pellet
por_b	0.5	Porosity of the bed (void/total)
rho_b	rho_p*(1-por_b)	Density of bed
MW_C3H8O3	92.09[kg/kmol]	Mol. wt. methane
MW_dee	118.1742[kg/kmol]	Mol. wt. hydrogen
MW_et	46.00995[kg/kmol]	Mol. wt. carbon dioxide
MW_feed	MW_C3H8O3*x_C3H8O3_feed+MW_et*x_et_feed+MW_dee*x_dee_feed	Mean molar mass of feed
x_C3H8O3_init	x_C3H8O3_feed	glycrol
x_dee_init	0.07	Ether feed mole fraction
x_et_init	0.86	Ethanol feed mole fraction
Dab_avg	0.00000000320797[m^2/s]	Average Bulk Diffusion Coefficient
eta_feed	-0.0084*T_feed[cP/K] +3.11441[cP]	
Cp_f_feed	6.6715*T_feed[J/(kg*K*K)]+1857.5	
kf_feed	-0.0002*T_feed [W/m/K/K] + 0.1807	
Re	G*dp/eta_feed	
D_ea_cons	0.000187[m^2/s]	Axial dispersion coefficient
kg_cons	0.276[m/s]	Particle-fluid mass transfer coefficient
k_ea_cons	34.1[W/(m*K)]	Axial thermal dispersion coefficient
hg_cons	7250[J/(s*(m^2)*K)]	Particle-fluid heat transfer coefficient
EGSR	58600[J/mol]	Activation energy for RGSR
AGSR	7.85e5[(m^6)/(kg*kmol*s)]	Pre-exponential factor for GSR reaction
MW_ga	MW_dee+MW_C3H8O3 - 2*MW_et	Molecular weight glycerol acetal
x_ga_feed	0	Mole fraction glycerol acetal
d_HR	20.65[kJ/mol]	Heat of reaction
Ci	rho/MW_feed	Total initial concentration
ci_C3H8O3	Ci*x_C3H8O3_feed	C3H8O3l initial concentration
Kcref	1250[kmol/m^3]	Equilibrium constant
Tref	298[K]	Temeprature reference
R	8.314[m^3*Pa/(mol*K)]	Gas constant
W_cat	1[kg/m^3]	Catalyst weight
n	-0.0004*T_feed^2[1/K/K] + 0.2324*T_feed[1/K]-32.794	Effectiveness factor

Appendix F: Simulation variable

c_et	(rho-mod1.C3H8O3*MW_C3H8O3 - mod1.dee*MW_dee-mod1.ga*MW_ga)/MW_et	
eta	(-0.0084)*mod1.Tf [cP/K] +3.1144[cP]	Fluid Viscosity
Cp_f	6.6715*mod1.Tf[J/(kg*K*K)]+1857.5	Fluid Heat Capacity
beta	G*(1-por_b)/(rho*dp*por_b^3)*(150*(1-por_b)*eta/dp+1.75*G)	Ergun Equation Constant
Sc	eta_feed/(rho*Dab_avg)	Schmidt Number
Sh	2+1.1*(Re^0.6)*(Sc^(1/3))	Sherwood Number
kg	Sh*Dab_avg/dp	Particle-Fluid mass transfer coefficient
Pem	1/((0.73*por_b/(Re*Sc))+(0.5/(1+9.7*por_b/(Re*Sc))))	Peclet Number - Mass transfer
D_ea	u*dp/Pem	Axial dispersion coefficient
kf	(1.355e-4)*mod1.Tf [W/m/K/K] + 0.0119	Fluid Thermal Conductivity
Pr	eta_feed*Cp_f_feed/kf_feed	Prandtl Number
Nu	2+1.1*(Re^0.6)*(Pr^(1/3))	Nusselt Number
hg	Nu*kf_feed/dp	Particle-Fluid heat transfer coefficient
Peh	1/((kp/(kf_feed*Re*Pr))+(0.73*por_b/(Re*Pr))+0.5)	Peclet Number - Heat transfer
k_ea	G*Cp_f_feed*dp/Peh	Axial Thermal dispersion coefficient
Dp_C3H8O3	((6e-22)[(m^2)/s])*(((mod2.Ts)/1[K])^5.127)	C3H8O3 diffusion coefficient in the pellet
Dp_dee	((2e-23)[(m^2)/s])*(((mod2.Ts)/1[K])^5.7458)	H2O diffusion coefficient in the pellet
Dp_ga	((2e-23)[(m^2)/s])*(((mod2.Ts)/1[K])^5.6728)	CO2 diffusion coefficient in the pellet
Dp_et	((2e-43)[(m^2)/s])*(((mod2.Ts)/1[K])^13.15)	H2 diffusion coefficient in the pellet
kGSR	AGSR*exp(-EGSR/R_const/mod2.Ts)	Rate constant for GSR
RGSR	kGSR*(mod2.C3H8O3p*mod2.deep-(1/Kc)*(mod2.etp)^2*mod2.gap)	Reaction rate
Conv_G	1-mod1.C3H8O3/ci_C3H8O3	Conversion Glycerol
Kc	exp(d_HR*(1/T_feed-1/Tref)/R_const)*Kcref	Equilibrium constant